Interfacing to Metal 3D Printed Micro-Gas Chromatography Columns

Capstone Report, Brigham Young University July 26th, 2021

James Harkness

Table of Contents

Table of Figures ----- 3
Abstract ----- 4
Chapter 1—Introduction ----- 5
1.1 Gas Chromatography ----- 5
1.2 Micro-GC ----- 6
1.3 3D Printing ----- 6
1.4 Project Design and Interfacing Study ----- 7
Chapter 2—Methods ----- 9
2.1 Sintering and Infiltration Furnace Process ----- 9
2.2 Stainless-Steel Capillary ----- 9
2.3 Capillary Interfacing Methods ----- 10
2.4 Powder and Binder Jet Printing Process ----- 10
Chapter 3—Results and Discussion ----- 12
3.1 Main Objective and Overview ----- 12
3.2 Bronze as Infiltrant ----- 15
3.3 Interfacing Methods ----- 17
Chapter 4—Conclusion ----- 23
Chapter 5—References ----- 25

List of Figures and Tables

Figure 1—Furnace used for this experiment. Fans visible under both ends used for cooling---------9
Figure 2—Electron microscope image of sintered stainless-steel powder----------14
Figure 3—Image of cross-section of hole in printed part for ferrule with taping for screw ----------16
Table 1—Percent weight copper in nine areas----------18
Figure 4—Image of part used for EDX analysis----------18
Figure 5—Images of cylindrical capillary test----------19
Figure 6—Sacrificial structure Joiner test ----------20
Figure 7—Sacrificial Powder Joiner test ----------21

Abstract

Metal 3D binder jet printing is being explored for micro-gas chromatography column fabrication. The binder jet printed parts are further processed by bronze infiltration to reduce porosity. Bronze infiltration also serves to create a gas-tight interface between the 3D printed columns and capillary tubing which is inserted into the printed part before sintering and used for fluid connection to other instrumentation. To control bronze infiltration, two porous sacrificial structures were explored: printed structures and sacrificial powders. The various interfacing methods were tested by pressurizing the capillary tube with 20 psi of argon while underwater to detect leaks between the capillary tube and the printed part. With the printed sacrificial structures, we frequently saw plugging of the capillaries. With sacrificial powder, plugging was not observed. We designed a structure to test sealing in the sacrificial powder process that resulted in gas-tight connections without plugging the capillaries.

Chapter 1—Introduction

1.1 Gas Chromatography

Gas Chromatography (GC) is a process by which volatile molecules and compounds are separated for detection. Chemicals separable by GC can be found in food, fuel, weapons, pharmaceuticals, and even on other planets [1]. The ability to separate and identify these volatile molecules has important applications in security, health, safety, and research. In GC, the distinct volatility and mass of different molecules is used to create separations between them [2]. An analyte, composed of volatile gasses or liquids, is heated and carried through a narrow (typically 250μm diameter) channel by an innate gas such as helium or argon where it will dissolve into and out of a polymer coating called the stationary phase [3]. Molecular interactions will determine the amount of time that a molecule spends in the stationary phase and thus how long it takes for the molecule to traverse the length of the channel. Separated analyte peaks exit the channel at different times. Various types of mass spectrometry or other analytical techniques detect the presence of the analyte at the exit while measuring additional molecular characteristics.

A challenge limiting the reach of GC in many applications is portability. The average length of a traditional gas chromatography column is between 30 and 100 meters long. Columns consisting of coiled quartz capillary are uniformly heated in convection ovens to facilitate separations. Because of the length and heating requirements most GC units are large and power intensive. The length of the column also means that analysis can take as long as an hour to perform [4]. These limitations on the mobility and speed of analysis have caused researchers to consider faster, smaller, and less power intensive chromatography systems, typically known as micro-GC.

1.2 Micro-GC

For many decades, silicon has been the choice material for fabricating micro-GC columns. While silicon has excellent thermal properties and extensively developed lithography and etching techniques, it suffers from limited geometric flexibility, brittleness, interfacing difficulty, and a limited channel length because the designs are confined to two dimensions. Columns are made in silicon by etching them on wafers using wet or dry etching techniques. These etched channels are then sealed by bonding a second wafer over the etched face [5]. The cross-sectional geometry of these channels are entirely dependent on the etching technique. The cross-section of a wet etch is roughly a semi-circle and the cross-section of a dry etch tends to be rectangular. These geometries leave corners where the polymer stationary phase could pool and cause uneven separations [4]. An additional challenge with silicon based micro-GC systems is the length of the columns. Micro-GC systems tend to have column lengths ranging from tens of centimeters up to a couple meters [5]. This is much less than the 30 to 100 meters of a standard GC system. Decreasing length from standard GC systems to micro-GC systems causes micro-GC to suffer from comparatively poorer separations. Extending the length of a micro-GC column is difficult due to the constraints of working in only two dimensions on silicon wafers. Interfacing with the columns in silicon micro-GC systems is another challenge because silicon is brittle and not easy to machine or bond to. For these reasons, micro-GC is not as widely used as standard GC.

1.3 3D Printing

A unique approach which has the potential to overcome many of the challenges facing micro-GC, particularly systems etched in silicon, is 3D printing because of its geometric flexibility. This means that columns can have circular cross-sections which reduces the risk of uneven distribution of the stationary phase. A 3D printed channel is not confined to the 2D surface of a silicon wafer opening up the

possibility of increasing the potential length of the column dramatically. Microfluidics is a field which has greatly benefited from 3D printing technology [6]. Many lab-on-chip systems include 3D printed capillaries. Most of these systems, however, are printed in low temperature polymers, which are unacceptable for GC. These polymers are unstable to withstand temperature cycling from room temperature to 300℃, which is necessary for good separations, making them a poor choice for micro-GC.

While many 3D printing technologies are specific to polymers, binder jet printing is a method which can print in metals. Metals have high thermal conductivity and can undergo thermal cycling. Binder jet printing uses uniform layers of powder, upon which is deposited a polymer glue. The glue solidifies through the layers to create a “green” part. The green part is left in the bed of powder until the glue is cured. It is then removed and sintered. The heat of the sintering burns out the polymer. The final product has many of the bulk properties of the powder metal. We will use stainless-steel which is not brittle, can withstand a large range of temperatures, has high thermal conductivity, and is easy to machine [7]. This makes it an ideal choice for creating columns for GC.

1.4 Project Design and Interfacing Study

Our group has designed a micro-GC column as a 3D printed 316 stainless-steel (SS) block composed of a series of stacked layers containing interconnected columns (for additional information see [8]). To prevent porosity present in binder jet printed parts, the part will be infiltrated with bronze at high temperature. For some of the parts, sacrificial structures were printed with the design. The dimensions and placement of the sacrificial structures was to make it energetically favorable for the bronze to fill the structures before the column. Another infiltrant control method used was sacrificial powder [9]. The powder was put around the part after sintering and drew excess bronze away from the column.

One challenge facing micro-GC is the method of interfacing. Because our design is made of 3D printed SS and bronze, there are a couple interfacing methods that will be discussed. The bulk of the project focuses on finding the best method for interfacing with the afore mentioned design. Using a graphite ferrule to seal between a standard GC quartz capillary and the printed part was explored but determined to not be a good method for creating a seal without additional machining, something that we wanted to avoid to preserve column integrity. The main method investigated was using bronze infiltration to create a gas-tight interface between the 3D printed columns and capillary tubing which is inserted into the printed part before sintering and used for fluid connection to other instrumentation. To control bronze infiltration, two porous sacrificial structures were explored: printed structures and sacrificial powders. The various interfacing methods were tested by pressurizing the capillary tube with 20 psi of argon while underwater to detect leaks between the capillary tube and the printed part. With the printed sacrificial structures, we frequently saw plugging of the capillaries. With sacrificial powder, plugging was not observed. We designed a structure to test sealing in the sacrificial powder process that resulted in gas-tight connections without plugging the capillaries.

Chapter 2—Methods Create Process diagram

2.1 Sintering and Infiltration Furnace Process

The furnace process used for sintering and infiltration was the same. The part is placed into the furnace on a boat. The boat is moved into the center of the furnace at room temperature. Hydrogen gas was flowed at 200 sccm and argon gas was flowed at 1800 sccm to create a reducing environment. The argon flow was reduced to 500 sccm after ten minutes. Ads can be seen in figure 1, fans blew on either end of the quartz tube to reduce and control temperature while the furnace was heated to 1135℃ and allowed to rest at that temperature for twenty minutes. The hydrogen flow was cut off for the last five minutes and the argon flow was again set to 1800 sccm to remove hydrogen from the furnace. Upon completion, the sample is then moved by the transfer arm to the edge of the furnace where it cools for ten minutes. All gasses are turned off and the sample is removed from the furnace.

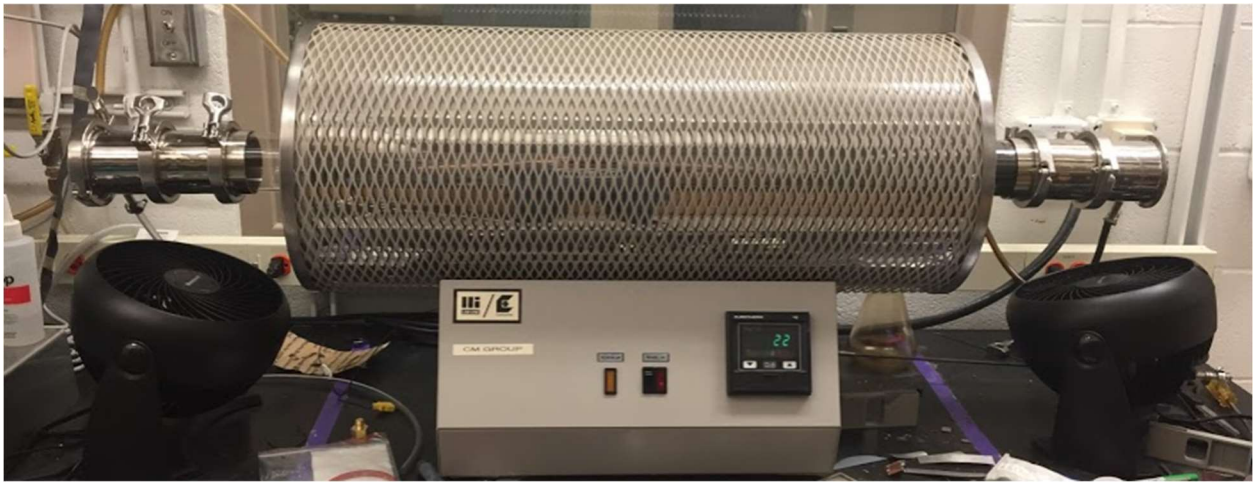


Figure 1—Furnace used for this experiment. Fans visible under both ends were used for cooling. When the sample had spent the required time in the furnace it was moved by the transfer arm to the right end of the furnace. There it cooled to approximately 200℃ and was removed from the furnace.

2.2 Stainless-Steel Capillary

Two sizes of SS capillary tubing were used for this experiment. McMaster-Carr Extreme-Pressure Miniature Stainless Steel Tubing with an inner diameter of 0.508 mm was used. This tubing is not standard capillary for GC but was purchased because of its low cost. The outer diameter was 1.524 mm which is much thicker than standard GC capillary. The thickness made the capillary easier to work with and more robust.

The other capillary size was Agilent's UltiMetal Plus Stainless-Steel Capillary Tubing. This capillary is a standard size for GC but was much more likely to get pinched in handling. The inner diameter is 0.53 mm with an outer diameter of 0.8 mm.

2.3 Capillary interfacing methods

Because of the difference in capillary sizes, different methods were used for connecting to gas for pressure testing. The standard SS capillaries were attached to a gas line via a standard GC joiner. The McMaster capillaries were first interfaced by inserting a 0.4 mm quartz capillary into the McMaster capillary and making the interface airtight with superglue. This proved to be messy and hard to recover the quartz capillary and unclog the McMaster capillary after testing. A new method was devised in which Blu-Tack was pressed around the interface of the McMaster capillary and quartz capillary. This sealing method was less gas-tight than the superglue but allowed for the quartz capillary to be removed and recovered.

2.4 Powder and Binder Jet Printing Process

Binder jet printing was done by an ExOne Innovent+. SS316L powder sieved for less than 20 µm diameter was used. The bed was placed in an oven at 400 ℃ for three hours for the glue to cure. Green

parts were extracted from the bed by brushes and air gun. The sacrificial powder was SS316 as well. The particle size was sieved for 150 µm.

Chapter 3—Results and Discussion

3.1 Main Objective and Overview

Several attempts were made to create an interface from 3D printed SS316 columns infiltrated with bronze to a standard quartz or SS GC capillary tube. Each one of these attempts will be discussed in detail. Preceding the discussion on the attempts at interfacing there will be a discussion on infiltration including the choice in material, sacrificial structures, and the theory behind infiltration as well as some discussion on sacrificial structure design.

3.2 Bronze as Infiltrant

3.2.1 Choice of Bronze as Infiltrant—Challenges and Solutions

10% weight tin Bronze was identified as a good candidate for infiltrating stainless-steel parts because of its low melting temperature (850℃) and high thermal conductivity. Sintering temperature used in our process reaches a maximum of 1165°C, which is well above the melting point of bronze, making it an appropriate temperature for infiltration as well.

Early attempts at infiltration were tried with a solid block of metal placed on top of the sample. Heating in the furnace melted the block and the molten metal flowed down into the part due to gravity and capillary forces. Control of the bronze by this method was difficult, however. Bronze occasionally flowed off the part and often flowed unevenly through it. It was found that the bronze would erode some of the printed part. This was due to absorption of steel by the bronze [10].

A solution to the negative effects of the bronze infiltration was found in using bronze powder instead of solid blocks. The powder could be poured into containers printed with the part, making it more easily contained. Runners or other structures between the container and the part allowed for the bronze to become saturated with steel and not damage the important features of the structure.

3.2.2 Infiltration Theory

The mechanism which drives infiltration is capillary action, which can cause infiltration in unwanted areas. Voids of many sizes in the stainless-steel matrix are filled with bronze. It was realized that capillary action can draw bronze not only through the holes in the matrix but also through the columns, plugging them and rendering them useless. Much of the work by the BYU team on this project has focused on how to prevent the bronze from filling columns and other necessary structures [9]. The height to which capillary action draws a liquid through a cylindrical void is given by the equation

$$h = \frac{2T\,cos\theta}{\rho g r} \tag{1}$$

where T is the surface tension, ρ is the density of the fluid, g is the gravitational force, r is the radius of the cylinder, and θ is the angle of contact between the liquid and the cylinder. Considering that the height has an inverse relation with the radius of the cylinder, one can assume that a fluid will fill a void of lesser cross-sectional area to a greater height than one with a larger cross-sectional area.

3.2.3 Sacrificial Structures

Following the hypothesis that infiltrant will fill voids of smaller cross-sectional area to greater heights, it is assumed that the infiltrant will preferentially fill the voids in the stainless-steel matrix before filling capillaries. Gaps in the matrix are microns wide (see figure 2) and capillaries are 500 µm diameter.

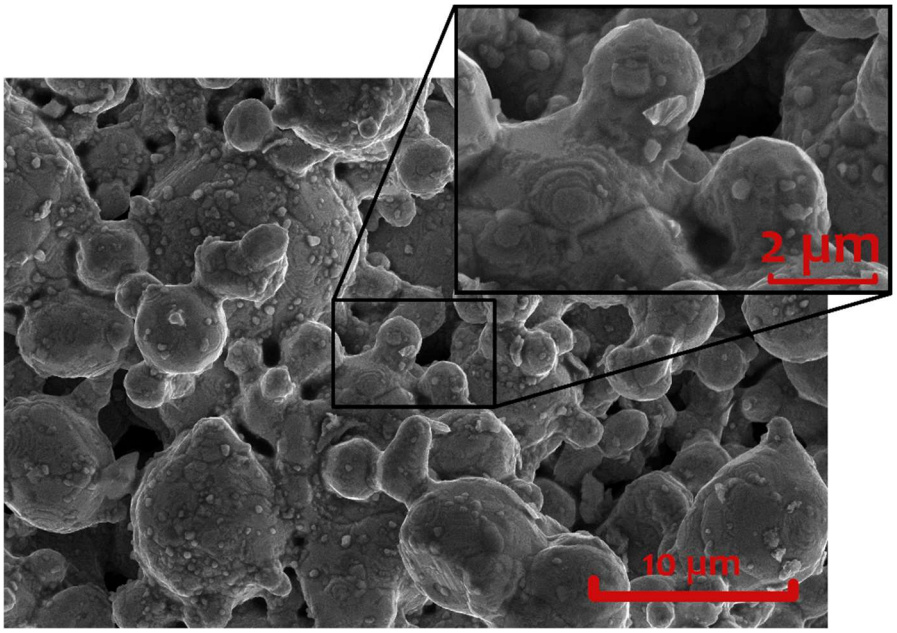


Figure 2—Scanning electron microscope image of sintered stainless-steel powder. The general gap size was observed to be in the 2 micron range.

The column capillaries however must not fill with infiltrant. Sacrificial structures are spaces designed to have a lesser cross-sectional area than that of the capillaries but more than the gaps between particles. Sacrificial structures were designed to be more energetically favorable to fill with excess bronze than larger capillaries. By this method bronze could be diverted away from important structures.

This hypothesis has been verified by work in our team at BYU [9]. I will describe this briefly as follows, a sacrificial structure test was designed. The part printed for the test had a wall perforated with holes of three different sizes, 250µm, 500µm, and 1mm, and two different geometries, square cross section and circular. The part was infiltrated with bronze. It was observed that the 250µm holes filled from the bottom to the top consistently. The 500µm and 1mm holes never filled all the way up to the top. The 1mm holes consistently filled to a lower height than the 500µm holes.

3.3 Interfacing Methods

3.3.1 Constraints

The interface between the GC column and the rest of the system is a very important part of GC because an improper interface can introduce impurities or disrupt the signal. In standard GC, graphite ferrules are used to seal around quartz capillaries. Graphite is desirable as a sealant because it will not absorb the analyte. The molecules that make up the analyte are volatile molecules and will thus absorb into any polymer present. Absorption of analyte causes peak tailing which decreases the resolution of the chromatogram. That is why silicone O-rings are not used in GC. As described above, many µGC systems are created by etching silicon wafers. Interfacing with a channel in a wafer is difficult without the use of polymer adhesives or seals. Silicon is not easily bonded or brazed to. This is a challenge facing the µGC community. Any polymer or dead space could be a place for analyte to pool, distorting the signal [5].

Our approach to µGC is unique because it is 3D printed metal. With bronze infiltrant to fill in any gaps, our parts are nonporous. Metal is also easy to machine and braze to. That means that interfaces can be made with no polymers and if engineered correctly they can leave very little dead space.

Because µGC requires capillaries of 500µm diameter, drilling and machining around the capillaries are impractical because of the potential for metal shavings or oil to slip down into the capillaries.

3.3.2 Ferrule Method

The first method that was attempted for interfacing was an imitation of the method used on standard GC systems: using a graphite ferrule. A block was printed and infiltrated which had a cavity of the proper dimensions to fit a ferrule and a screw for tightening. After infiltration, the hole was tapped. A ferrule

was inserted into the cavity with a standard 460µm capillary tube inserted. The capillary screw was inserted and tightened by wrench. The capillary, which extended out of the device through a hole in the screw, was attached to a standard GC connector and pressurized to 20psi with argon. See figure 3. The apparatus was submerged in water so that any leaks would be observed. This test was repeated multiple times and once even with an infiltrated but not sintered piece. Each test was unsuccessful in preventing leaks. In the uninfiltrated test the argon was shown to have percolated out through the printed stainless-steel matrix as well as apparently flowing around the ferrule. The other tests leaked around the ferrule as well though not through the printed part. This shows the necessity of infiltration for creating air-tight parts.

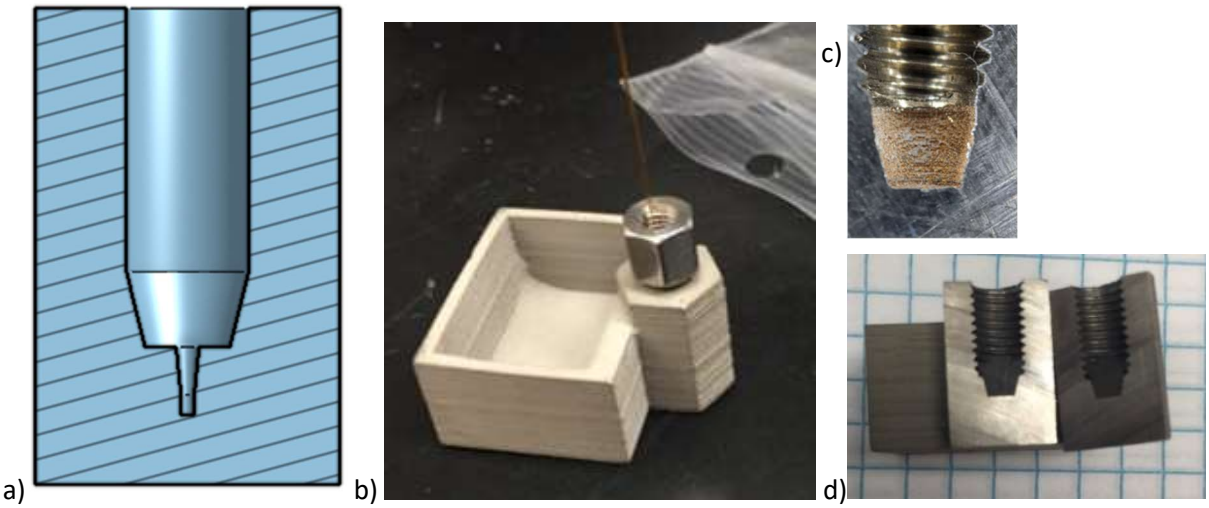


Figure 3—a) Schematic of ferrule hole, b) Ferrule inserted with screw and capillary, c) Image of cross-section of hole in printed part for ferrule with taping for screw, d) Cross-section of ferrule hole with ferrule. This part was sintered but not infiltrated and thus lost gas through the pores in the printed part as well as through the seal.

The failed parts were cross sectioned. The cross sectioning showed that the ferrules were not capable of creating an airtight seal against the printed and infiltrated metal. Surface roughness was approximated at ±50µm. Under typical conditions, the ferrule seals against a machined surface with very few surface

defects. With the large defects of the printed part, it was unable to deform to create an adequate seal. The design was determined to be ineffective, and alternatives were researched.

3.3.3 Direct Steel Capillary Method

Introduction

It was decided that sintering the printed part with a capillary tube inserted into a cylindrical hole could be an effective sealing method. A cylindrical cavity, several millimeters deep, with the cross-sectional area of the capillary was be printed and the capillary was inserted before sintering. The parts were sintered together. During infiltration, it was hoped that the bronze would wet to the outer surface of the capillary and bridge any gaps between the steel capillary and the printed steel matrix. This would create an airtight seal between the printed column and the steel capillary, effectively brazing the capillary to the part.

Infiltration Study for Placement of Capillary

It was relevant for my design to determine if gravity had a large effect on the level of infiltration over various heights. If it did, this would restrict the places where a standard GC capillary could be successfully joined with the printed column. To determine this, I used one of my printed parts which had ha height of 7 mm. One face of the part was polished and sectioned off into nine parts with a diamond scribe as is shown in figure 4. Energy-dispersive X-ray Spectroscopy (EDX) was used to determine the percentage of copper over a 200 μm^2 area. If the percentage of copper was higher in the lower three sections than the top three, then it would be determined that gravity does have an effect over 7 mm height differences.



Figure 4—Image of part used for EDX analysis. The part was sanded, polished, and then sectioned into nine parts with a diamond scribe as can be seen in the image.

	Left	Center	Right
Top	11.4 ±0.6%	14.0 ±0.6%	19.0 ±0.7%
Middle	13.8 ±0.9%	13.6 ±0.8%	16.9 ±0.8%
Bottom	15.1 ±1.1%	14.2 ±0.7%	12.0 ±1.0%

Table 1—Percent weight copper in nine areas measured using energy-dispersive x-ray spectroscopy.

Results shown in table 1 indicate that there was variation in the copper percentage throughout the piece, but that it did not correlate with the height of the area scanned. This suggests that a capillary tube inserted near the top of the piece would be as likely to form a gas-tight seal from bronze infiltration as a one inserted near the bottom.

Capillary in Cylinder Method

The first test of this design consisted of a dead-ended hollow cylinder into which the capillary would be inserted. See figure 5. The end of the cylinder was blocked to prevent air flow through. Around the cylinder was a box into which bronze powder would be placed for infiltration. The test was to determine if the seal could hold air. The apparatus would be submerged and put under 20psi of argon.

There were two attempts at this design, only one of which held air. For the failed test, the bronze did wet to the capillaries making an effective bond between the two parts, but the bond was not airtight. The part that did hold air had infiltrant in the capillary, meaning that the test was a false positive. The bronze in the capillary was determined by putting a wire down the capillary to determine the length. When the length of the inner capillary was compared with the length cut, it was realized that several millimeters of the capillary was plugged with bronze. A better test was determined to be one where there was an inlet and outlet. If argon could flow through the capillaries while open and would not leak when the outlet was closed, this would be deemed a successful experiment.

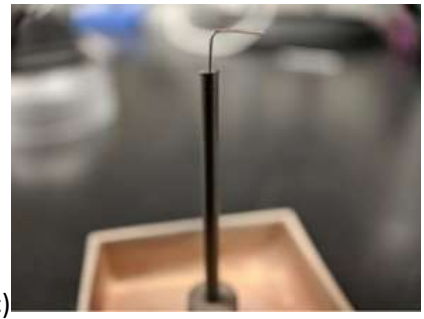
a)  b)  c) 

Figure 5—Images of a dead-ended cylindrical capillary test. a) sintered part with capillary inserted and bronze powder in container, b) post infiltration, c) using a wire to check for infiltrant blocking the capillary.

Double Capillary—Printed Sacrificial structures

A test was designed to join two stainless-steel capillary tubes using a printed metal part (See figure 6). The printed part in this test was a proxy for connection ports on a printed micro-GC column. The printed part with capillary tubes inserted was sintered and infiltrated. Argon from a tank with a regulator set at 20 psi was connected to one of the capillaries. The fluid connection to the part was deemed a success when the argon flowed through the capillaries and joiner without leaks. In a second test, the capillary

was plugged at the exit to see if the pressurized joiner and capillaries would leak. Sacrificial structures printed as part of the piece were used to control bronze during infiltration.

Two capillary tube sizes were used, and corresponding holes to match the tube outer diameter (OD) were printed. The 1.65 mm holes were designed and printed to accept the McMaster size tubing (1.524 mm OD) and 1 mm diameter holes were designed and printed for the Agilent size tubing (0.8 mm OD). The McMaster tubing was a tight fit, requiring twisting and applying some force by hand in order to insert into the printed hole. On the other hand, the Agilent tubing slid easily into the hole with very little force and without twisting. The McMaster capillary insertion process resulted in loose powder in the printed capillary (observed visually) which could be removed by lab air.

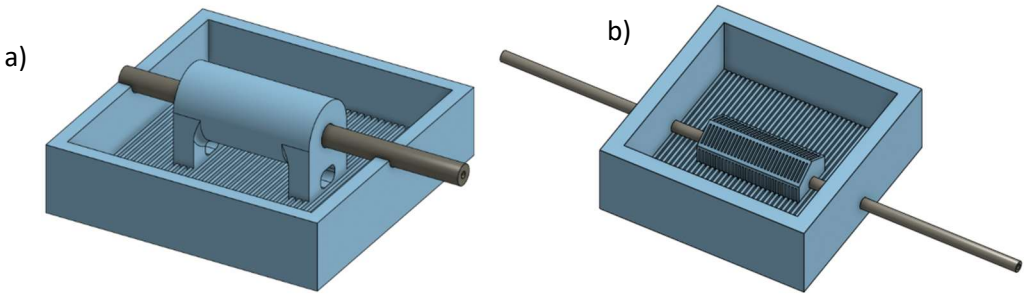


Figure 6—CAD model of sacrificial structure joiner tests. a) Two capillary tubes (shown in grey) are inserted into the concentric holes on each side of the horizontal cylinder in the 3D printed part (shown in blue). Capillary tubes do not completely meet in the part but are separated by a printed capillary of length 0.5 mm and diameter 0.5 mm. Ridges in the base of the printed part serve as sacrificial structures for controlling bronze infiltration. The sacrificial structures have ridges that are 0.35 mm high separated by 0.25 mm gaps. The sacrificial void volume for this structure was 53.55 mm^3. b) A second joiner test had a slightly different geometry containing sacrificial ridges in the base that were 0.45 mm high separated by 0.15 mm gaps. Sacrificial structures of the same geometry were also placed around the joining section. The sacrificial void volume for this structure was 38.59 mm^3.

There were two variations on sacrificial structures tried with this test. The first incorporated ridges 0.35 mm tall and with 0.25 mm gaps between. The ridges ran the length of the base and provided 53.55 mm^3 total sacrificial void space (Figure 6a). Four tests were conducted with the 0.25 mm gap design. All of them resulted in capillaries filled with bronze. A second test was designed (figure 6b) with a 0.15 mm gap between ridges. It was hypothesized that the smaller gap would result in greater capillary forces and

prevent bronze from flowing into the capillary tubes. The second test incorporated ridges 0.45 mm tall and with 0.15 mm gaps. This design gave 38.59 mm^3 total sacrificial void space. Ten tests were attempted with the two capillary tube sizes. Of six McMaster tube tests, four were blocked. Two McMaster tube tests remained unblocked but showed bubbles escaping at the interface with the printed part when the exit was blocked. Of four Agilent capillary tube tests, three were blocked. One remained unblocked but showed bubbles escaping at the interface with the printed part when the exit was blocked.

Double Capillary—Sacrificial Powder

A design which incorporated sacrificial powder instead of printed sacrificial ridge structures was also tested. This design had a cylindrical joiner that was surrounded by sacrificial powder as shown in figure 7. A new area was needed for the bronze reservoir and so the structure was expanded to contain a separate chamber for bronze powder. This design featured the same designed and printed hole sizes, to accept McMaster and Agilent tubes, as the previous test.

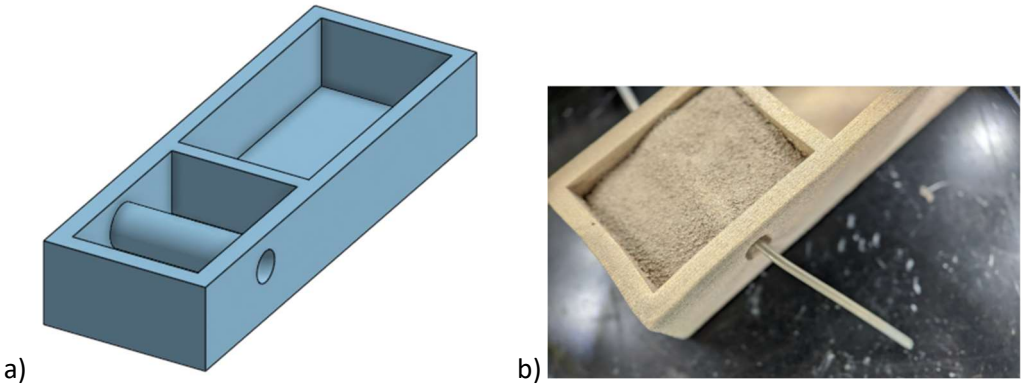


Figure 7—Sacrificial Powder Joiner test. Rectangular chamber towards the back is for holding bronze powder. Area around the cylindrical joiner is where the sacrificial powder is placed. a) CAD design of the printed part; not shown are the capillary tubes that would be inserted into the joiner from either end. b) Part with capillary tubing after printing, sintering, and infiltrating with bronze. Capillary tubing droops during processing and is also easily bent as seen in image. Slight bending of capillary tubing does not impede flow.

The sacrificial powder void volume was 339 mm^3 in volume. This is calculated as 58% of the total powder volume (see [8]). Nine tests were performed with sacrificial powder for bronze control. All of the tests were observed to have clear capillaries after infiltration (the excess powder created from insertion of McMaster capillaries had been removed following tube insertion using lab air). Four of the tests used McMaster capillary tubes. All of these McMaster capillary tests remained unblocked and did not show bubbles when the exit was blocked! Five of the tests were with Agilent capillary tubing. Upon visual inspection all of the Agilent test samples remained clear of bronze. Four of the Agilent tests leaked when the exit was blocked (the fifth could not be hooked up for pressure testing because the capillary was cut too short).

Chapter 4—Discussion and Conclusion

Interfacing tests using a ferrule leaked profusely for each of the tests. The surface roughness of the printed part was determined to be the cause of leaking. Graphite ferrules were incapable of forming to the many bumps and surface features that are inherent with binder jet printing. This is not surprising because the intended use of the graphite ferrules is in a machined joiner. We considered machining our printed part to match a GC joiner. This route of research was forgone in favor of the capillary study because machining a part in near proximity to a 0.5 mm capillary opening in the printed part could cause shavings or oil to be dropped down into the hole which may compromise column integrity.

The double capillary tube tests with 0.25 mm gap width sacrificial structures all had capillary tubes fill with bronze. We believe the 0.25 mm sacrificial structures were too large to effectively prevent infiltrant from being drawn into the capillary tubes. Davis et. al. describe the role of the void size of sacrificial structures on infiltration control. The tests with 0.15 mm gap width sacrificial structures were better at preventing the tubes from filling, but only for three of the ten tests indicating that the 0.15 mm voids still are too large for high yield fabrication of gas ports. Of the three that remained clear, there were still leaks when the part was put under higher gas pressure by blocking the exit. We attribute this to using an insufficient amount of bronze powder.

Every test with sacrificial powder resulted in clear capillary tubes. We roughly estimate the void size in the sacrificial powder to be around ten microns. We attribute the lack of plugged parts to this much smaller void size. All of the four McMaster capillary tube tests were successful at holding 20 psi of argon when the exit was sealed. None of the Agilent tubing was sealed to with a gas-tight seal. We attribute this to the loose fit of the printed part around the tubing when it is inserted for sintering. The McMaster tubes fit tightly into the printed parts and resulted in no leaks when sufficient bronze was used, as was

done in all sacrificial powder tests. We believe that printing a hole for the Agilent tube to fit as tightly as the McMaster tubing would result in gas-tight seals to the Agilent tubing.

Of the three tests, the sacrificial powder test had the most void volume at 339 mm^3. It also resulted in no plugged samples, but the success of a given test may not be determined by void volume alone. The test with the 0.15 mm gap size sacrificial structures had approximately three quarters of the void volume of the 0.25 mm gap test but produced more capillaries that were not blocked. Gap sizes in the sacrificial powder are likely on the scale of ten microns. This suggests that the most important feature for preventing capillary tubes from filling may be the gap size and not the total void volume. We realize that there is a fair amount of variation under some of the repeated test conditions. Further testing to provide some validation to this theory would be to use a reduced amount of sacrificial powder and observe if the same results are obtained.

Our conclusion is that inserting tubes into cylindrical holes in printed parts before sintering and infiltrating with a sacrificial powder for control of bronze infiltrant may be an effective method for interfacing with 3D printed metal columns for micro-GC.

Chapter 5—References

[1] Navarro-González, R., Navarro, K. F., de la Rosa, J., Iñiguez, E., Molina, P., Miranda, L. D., ... & McKay, C. P. (2006). The limitations on organic detection in Mars-like soils by thermal volatilization–gas chromatography–MS and their implications for the Viking results. *Proceedings of the National Academy of Sciences*, *103*(44), 16089-16094.

[2] Rahman, M. M., Abd El-Aty, A. M., Choi, J. H., Shin, H. C., Shin, S. C., & Shim, J. H. (2015). Basic overview on gas chromatography columns. *Analytical Separation Science*, 823-834.

[3] Abraham, M. H., Poole, C. F., & Poole, S. K. (1999). Classification of stationary phases and other materials by gas chromatography. *Journal of Chromatography A*, *842*(1-2), 79-114.

[4] Juvet, R. S., & Dal Nogare, Stephen. (1964). Gas Chromatography. *Analytical Chemistry*, 36(5), 36–51. https://doi.org/10.1021/ac60211a003

[5] Ghosh, A., Vilorio, C. R., Hawkins, A. R., & Lee, M. L. (2018). Microchip gas chromatography columns, interfacing and performance. *Talanta*, *188*, 463-492.

[6] Bhattacharjee, N., Urrios, A., Kang, S., & Folch, A. (2016). The upcoming 3D-printing revolution in microfluidics. *Lab on a Chip*, *16*(10), 1720-1742.

[7] Mostafaei, A., Elliott, A. M., Barnes, J. E., Li, F., Tan, W., Cramer, C. L., ... & Chmielus, M. (2021). Binder jet 3D printing—Process parameters, materials, properties, modeling, and challenges. *Progress in Materials Science*, *119*, 100707.

[8] Kohls, I. (2021). Fabricating Micro-Channels using 3D Printing and Infiltration, BYU Senior thesis

[9] Davis, D, Harkness, J, Kohls, I, Crane, N, Jensen, B, Vanfleet, R, Davis, R. (2021). Pressure Control during Bronze Infiltration of Binder-Jet Printed Stainless-Steel to Create Metal Microchannels.

[10] Ziaee, M., & Crane, N. B. (2019). Binder jetting: A review of process, materials, and methods. *Additive Manufacturing*, *28*, 781-801.